POROSITY ANALYSIS VIA 3D SERIAL SECTIONING FOR ADDITIVELY MANUFACTURED ALLOY SAMPLES

Veeraraghavan Sundar, Satya Ganti, Bryan Turner
UES Inc., 4401 Dayton Xenia Rd., Dayton, OH 45432

Keywords: Serial Sectioning, Three Dimensional (3D) Microstructure, Porosity, Stereology, Automated Serial Sectioning, Robo-Met.3D, Porosity, Additively Manufactured Alloys, 3D Reconstruction

Introduction

Additive manufacturing (AM) processes allow components to be directly produced from computer aided design (CAD) models by dividing them into thin two dimensional (2D) slices, which are built sequentially on top of one another [1]. Porosity plays a critical role in determining the mechanical behavior of additively and conventionally manufactured metal components. Defects such as voids decrease the strength and fatigue life of these components, which can limit the application of AM.

Until the advent of serial sectioning, classical stereological methods that extrapolate information from 2D images were used to quantify porosity from microstructural analyses. The underestimation of pore sizes that results when only a 2D section through a porous body is measured is illustrated by the sketch in Figure 1. For any given pore that is intersected by a plane, only rarely will the plane intersect the pore at a true diameter and in most cases, the plane will intersect at a section through the pore where the diameter of the exposed circle of intersection is smaller than the true diameter of the pore.

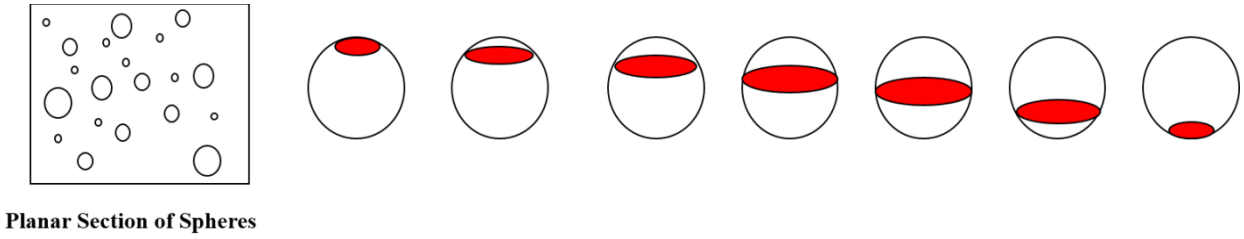

Figure 1: 2D Sections Through a 3D Distribution of Pores

Serial sectioning involves removing material from a sample layer by layer – in a sense, the inverse of additive manufacturing. The sample is ground, polished, optionally etched and the layered sections are imaged using optical microscopy [2,3]. Arrays of image tiles from each layer can be stitched into montage or mosaic images. Stacks of such images are then aligned and analyzed using open source or commercially available image analysis software to create a three dimensional (3D) dataset. Serial sectioning is a practical and direct method of obtaining 3D microstructures, especially when automated [4].

In this study, we used the Robo-Met.3D® system to investigate the quantification of porosity in additively manufactured and conventional alloy components. Robo-Met.3D is a fully automated serial sectioning system that generates 2D optical microstructural data for 3D reconstructions. Common applications of Robo-Met.3D include studying additively manufactured components [5], analysis of welds and thermal barrier coatings [6], and fiber orientation effects in ceramic matrix

composites [7]. Recent studies suggest some advantages of this method over nondestructive methods such as laser ultrasound and micro-CT evaluations [8].

Materials and Methods

Material Composition and State

Two samples manufactured by electron beam powder bed fusion (EPBF) and a conventionally processed sample, were analyzed for this study. A fourth sample manufactured by laser powder bed fusion (LPBF) with hot isostatic pressing (HIP) was also analyzed, in less detail. The samples are described in Table 1. Samples were excised from larger component builds, and were conventionally mounted in metallographic mounts (~38mm diameter x 25mm height) for automated serial sectioning.

Table 1: Serial Sectioning Samples and Processing

Composition	Abbreviated Label	Manufacturing Method	Post Processing
Ti 6Al 2Sn 4Zr 2Mo	Ti6242	AM - EPBF	None
Ti 6Al 4V	Ti64	AM - EPBF	None
Inconel 100	IN 100	Forged at 1163C	Heat treated: 1205C /3 min
Inconel 718	IN 718	AM - LPBF	HIP

Grinding and Polishing for Serial Sectioning

A typical automated grinding and polishing program for materials of this type involves diamond suspensions of varying sizes – 9, 6, 3 and 1 microns, and finishing with 0.05 microns colloidal alumina or silica. Polishing times may be varied automatically to achieve varying rates of material removal. The IN 100 sample was etched with Kalling's reagent to enhance contrast, while the others were examined as polished. Intermediate and final cleaning steps with water and ethanol are programmed in to keep cross contamination to a minimum.

Image Acquisition and Processing

Optical images were automatically acquired with the Zeiss Axiovert microscope built into the Robo-Met.3D system. The 2D image tiles from each layer were stitched into montages, registered with the images from the next layer using Fiji software. Acquisition parameters are shown in Table 2.

Table 2: Serial Sectioning Data Acquisition Parameters

Material	Overall Magnification	Resolution in x-y (microns)	Sectioning Rate (microns/section)	No. of Sections Analyzed	Dimensions Analyzed (microns)
Ti6242	100X	1.08	5.5	70	3000x4500x385
Ti64	100X	1.08	2.3	150	3439x1590x345
IN 100	100X	1.08	2.0	120	1000x1000x240

Results

Linearity of Material Removal Rate

Robo-Met.3D uses z-focus or z-height of the optical microscope for accurate material removal measurements between sections, rather than fiducial marks. The accuracy and repeatability of serial section thickness is maintained by careful control of polishing parameters and times. As shown in in

Figure 2, a highly linear material removal rate of between 1.9 and 5.4 microns was maintained for all materials.

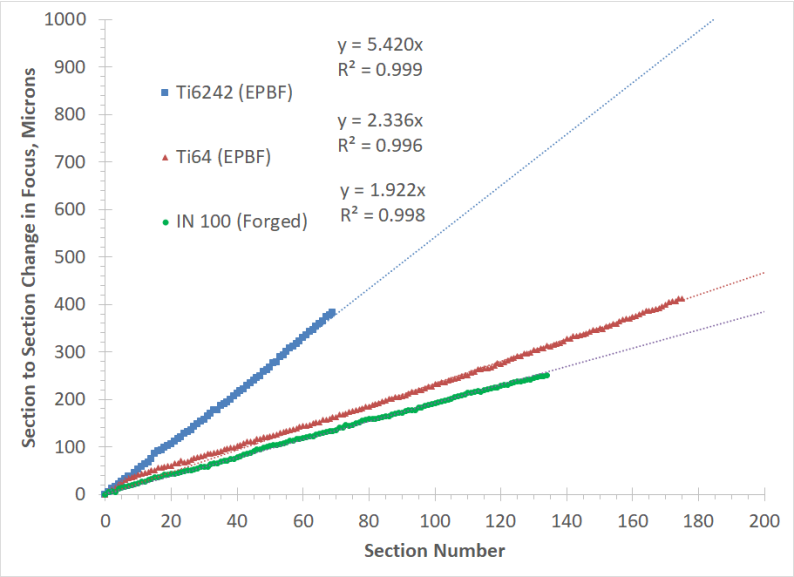

Figure 2: Linear Robo-Met.3D Material Removal Profiles

Single Slice and 3D Renderings

Binary images for 2D analysis were made by selecting pixel intensity threshold using Fiji/ImageJ. These images were stacked and aligned using Fiji. 2D images and segmented renderings for each material are shown in in Figures 3-5.

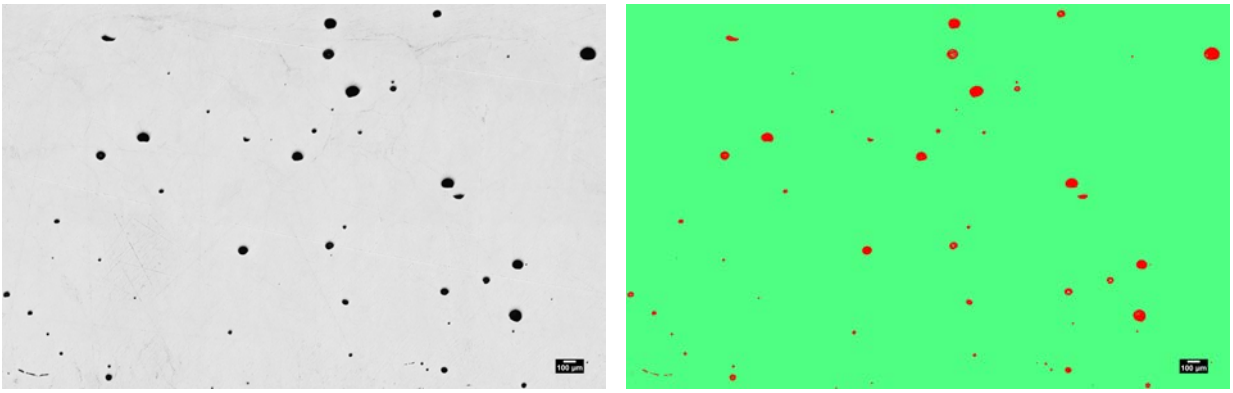

Figure 3: 2D Microstructure and WEKA Segmented Image for Ti6242

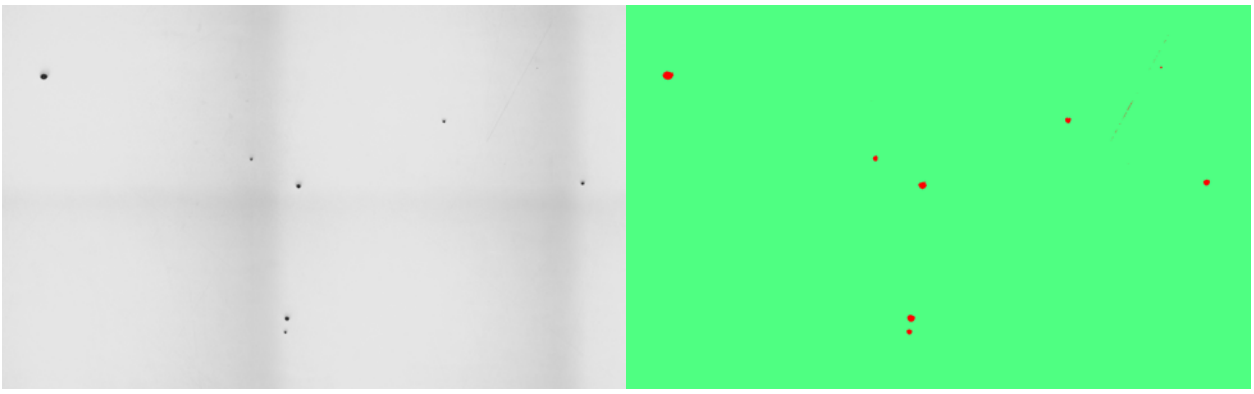

Figure 4: 2D Microstructure and WEKA Segmented Image for Ti64

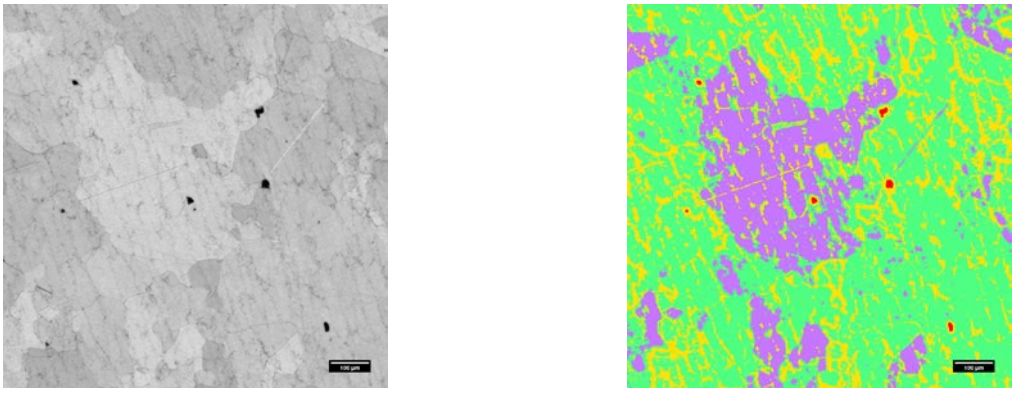

Figure 5: 2D Microstructure and WEKA Segmented Image for IN 100

Next, 3D datasets were reconstructed and visualized in 3D using Image-Pro Premier 3D software, version 9.3. The resultant 3D renderings for the three un-HIPed materials are shown in Figures 6, 7 and 8.

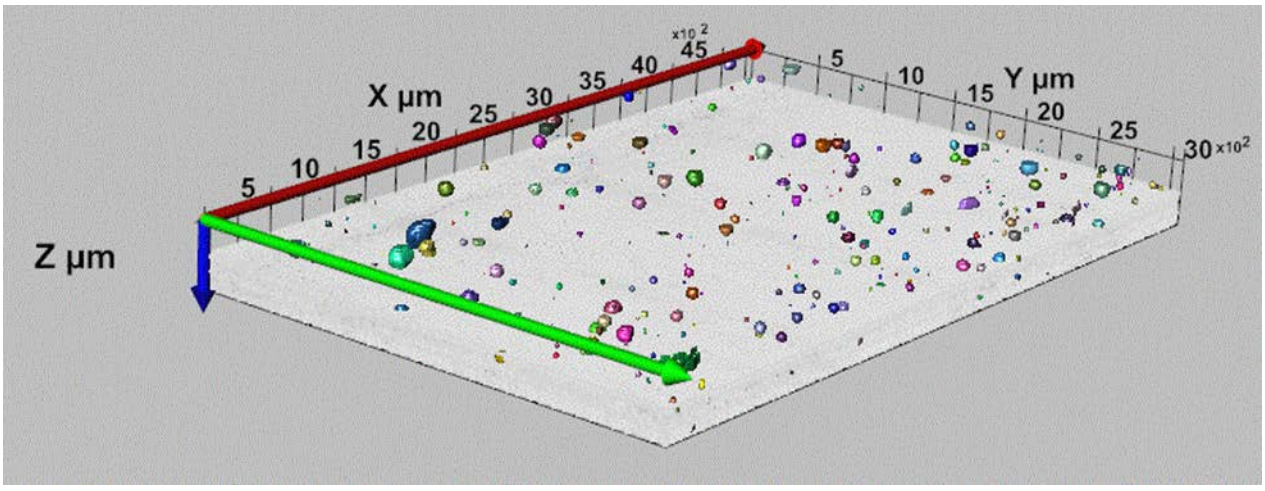

Figure 6: 3D Microstructure and Porosity Distribution for Ti6242

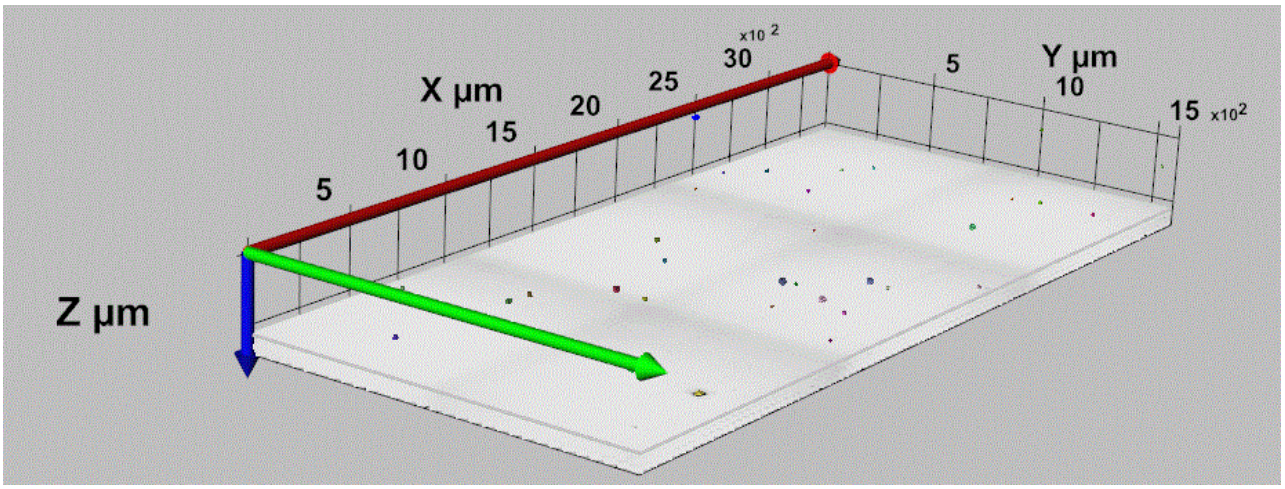

Figure 7: 3D Microstructure and Porosity Distribution for Ti64

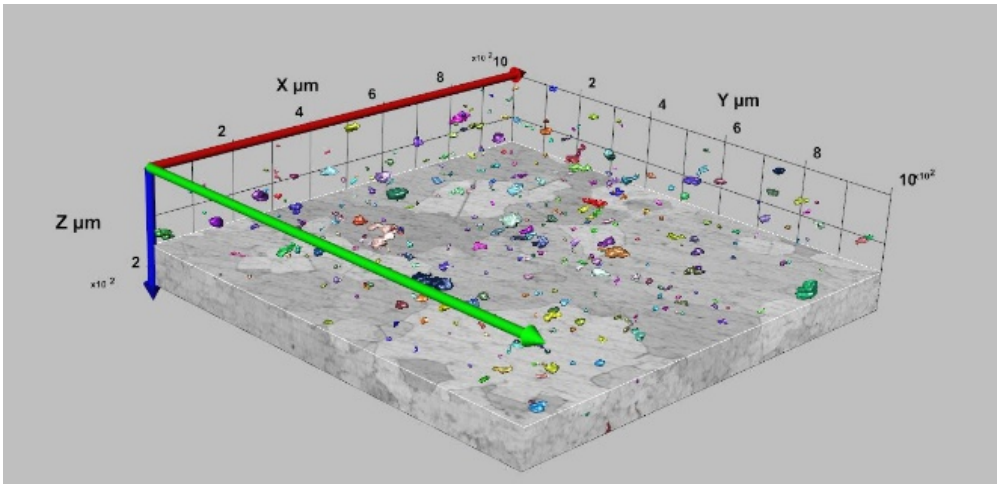

Figure 8: 3D Microstructure and Porosity Distribution for IN 100

We compared Robo-Met.3D direct measurements of the pore size distribution in a volume of material in 2D based on classical stereology and in 3D based on direct observation of the volume. For selected sections in the volume analyzed, equivalent spherical diameter (ESD) was calculated, and compared to the volumetric porosity average calculated from the entire 3D volume.

Hot Isostatically Pressed IN 718 Sample Results

As expected, few pores were discovered in the HIP-ed sample, and it is treated separately from the two AM and one conventional sample with a larger incidence and distribution of pores. Over 250 sections were collected for the HIP-ed IN 718 LPBF sample, with an average removal rate of about 14.6 microns per section. An overall magnification of 50X, with x-y resolution of 2.1 microns, was obtained. Only 50 slices with observed defects were used in the analysis, for a volume analyzed of 3058x8104x745 microns. Representations of 2D and microstructures for the IN718 sample are shown in Figure 9. The types of porosity uncovered in this sample are consistent with lack of fusion defects, based on position and shape.

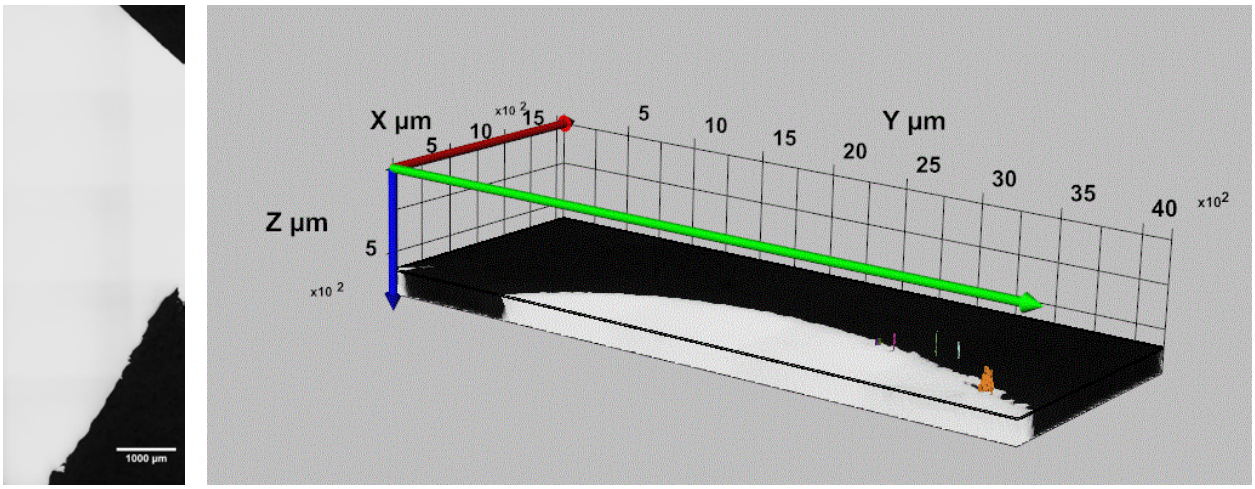

Figure 9: Two (left) Versus 3D (right) Microstructure with Lack of Fusion Defects for IN718

Discussion

3D Porosity Statistics

The pore size distribution from the complete 3D experimental datasets captured with Robo-Met.3D are shown in Figure 10. The 3D results for each material are summarized in Table 3.

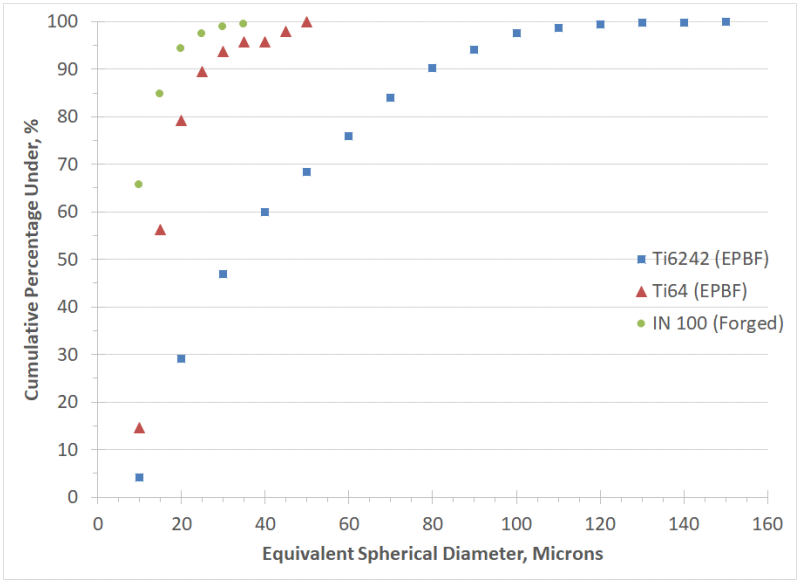

Figure 10: 3D Pore Size Distribution for Ti6242, Ti64, IN 100

Table 3: 3D Porosity Statistics for Samples, Microns

Material	Minimum	Maximum	Mean	25th Percentile	Median	75th Percentile
Ti6242	5.5	149.7	40.1	17.8	31.4	58.9
Ti64	8.69	47.0	16.4	11.6	13.9	18.5
IN 100	5.1	37.1	10.3	7.05	8.5	11.7

Variability in 2D Analyses

Beyond the descriptive statistics that are captured well by the 3D analysis, it is useful to compare the current 2D methods, where porosity is extrapolated from a single slice, to the complete 3D volume description. In order to do this, several regularly spaced slices were selected in each sample. A single slice would present only a limited cross section of the sample. The variation in the porosity measure calculated from each 2D slice is significant, as illustrated in Figure 11.

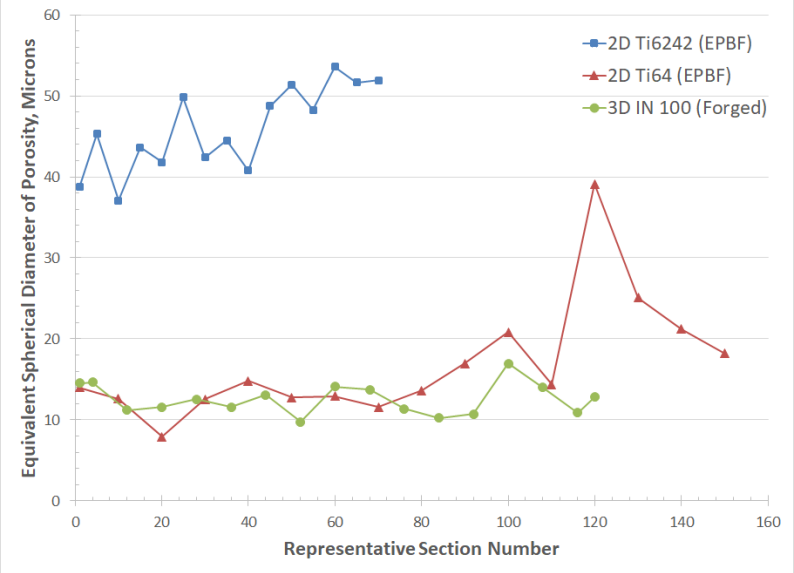

Figure 11: 2D Slice-to-Slice Variability in Pore Size

For the Ti6242 sample, the minima and maxima of estimates based on analysis of a single slice varied from -19 % to +17% below and above the mean of the 2D estimates, respectively. Using a similar approach, ranges of -53 to +133% and -23% to +35% were calculated for the Ti64 and the IN100 samples, respectively. All three samples were subjected to forming processes that induce anisotropy, and such variation is not surprising. However, this does highlight the need for more comprehensive estimates. Direct measurement provides accurate representation of features when measurement of porosity is a design optimization parameter and provides more reliable data to predict mechanical properties such as the fatigue life of additively manufactured parts.

Conclusion

In this analysis, three materials were successfully serial sectioned over large, representative volumes, for porosity analysis. A high level of linearity was achieved for material removal rates. Single 2D slices were analyzed for porosity, and were found to have high variability in porosity estimate results depending on which slice was analyzed. These results were compared to direct experimental measurements using Robo-Met.3D, which provided a more comprehensive estimate. The HIP-ed sample evaluated correlated with the expectation of lower porosity, and revealed lack of fusion defects. Visualization of the 3D microstructural and topological features using serial sectioning methods such as Robo-Met.3D creates a better understanding of the actual microstructural features. Such direct measurements provide accurate representations, which are imperative to correctly detect pores of critical size for fatigue life prediction, especially for additively manufactured parts.

Acknowledgements

We gratefully acknowledge the advice, guidance and input of Michael Uchic, Lee Semiatin (US AFRL), Dennis Dimiduk (Blue Quartz Inc.), John Porter and Bill Davis (UES).

References

[1] Sames, W. J., List, F. A., Pannala, S., Dehoff, R. R., & Babu, S. S. (2016). The metallurgy and processing science of metal additive manufacturing. International Materials Reviews, 61(5), 315-360.

[2] Voorhees, J. (2001). Quantitative Serial Sectioning Analysis. *Journal of Microscopy, 201*(3), 388-394.

[3] J.E. Spowart, H. M. (2003). Collecting and Analyzing Microstructures in Three Dimensions: A Fully Automated Approach. *The Minerals, Metals & Materials Society (TMS)*, 1- 6.

[4] DeHoff, R., 1983. Quantitative Serial Sectioning Analysis: Preview. *Journal Of Microscopy,* 131(3), pp. 259-263.

[5] Seifi, M., Ghamarian, I., Samimi, P., Collins, P. C., & Lewandowski, J. J. (2016). Microstructure and mechanical properties of Ti-48Al-2Cr-2Nb manufactured via electron beam melting. In *Ti-2015: The 13th World Conference on Titanium*.

[6] Madison, J. D., Huffman, E. M., Poulter, G. A., & Kilgo, A. C. (2015). *R3D at Sandia National Laboratories-A User Update* (No. SAND2015-7665PE). Sandia National Laboratories (SNL-NM), Albuquerque, NM (United States).

[7] Bricker, S., Simmons, J. P., Przybyla, C., & Hardie, R. (2015, March). Anomaly detection of microstructural defects in continuous fiber reinforced composites. In *SPIE/IS&T Electronic Imaging* (pp. 94010A-94010A). International Society for Optics and Photonics.

[8] Everton, S., Dickens, P., Tuck, C., Dutton, B., & Wimpenny, D. (2017). The Use of Laser Ultrasound to Detect Defects in Laser Melted Parts. In *TMS 2017 146th Annual Meeting & Exhibition Supplemental Proceedings* (pp. 105-116). Springer International Publishing.